The University of Osaka
Institutional Knowledge Archive

OUKA

Title	Experimental study of energy transport in thin Al and Au foils irradiated with a 263-nm laser
Author(s)	Tanaka, K.A.; Yamauchi, A.; Kodama, R. et al.
Citation	Journal of Applied Physics. 1989, 65(12), p. 5068-5071
Version Type	VoR
URL	https://hdl.handle.net/11094/2877
rights	
Note	

The University of Osaka Institutional Knowledge Archive : OUKA

https://ir.library.osaka-u.ac.jp/

The University of Osaka

Experimental study of energy transport in thin Al and Au foils irradiated with a 263-nm laser

K. A. Tanaka, A. Yamauchi, R. Kodama, T. Mochizuki,[a] T. Yabe,[b] T. Yamanaka, and S. Nakai

Institute of Laser Engineering, Osaka University, Suita, Osaka 565, Japan

C. Yamanaka

Institute for Laser Technology, Amagasaki, Hyogo 661, Japan

Irradiating an ultraviolet (uv) laser on aluminum (Al) and gold (Au) thin targets, emissions from the rear side of the targets were temporally resolved. A clear difference was observed between the above two targets. Given the fact that absorbed laser energy can be converted with a very high efficiency to soft x rays in a high-Z plasma, a characteristic emission peak only observed for Au targets was attributed to the effect of soft x-ray energy transport. The observed results were compared with those computed by a one-dimensional hydrodynamic simulation HIMICO. The ablation pressures estimated from the emissions indicate that the pressure scaling for Au is close to the one by x-ray drivers rather than by a uv laser.

I. INTRODUCTION

Short-wavelength lasers ($\lambda \leqslant 0.5\ \mu$m) have been proven to have ablation pressures significantly higher than the long-wavelength ($\lambda \geqslant 1\ \mu$m) ones[1] and to create little suprathermal electrons[2] deleterious for inertial confinement fusion. In addition, the soft x-ray conversion efficiency can become very high for a large atomic number (Z) target with a uv laser.[3,4] It thus becomes particularly important to understand the energy transport mechanisms highly weighted with x radiation in targets irradiated by a uv laser. A number of experimental and theoretical studies[5-13] delineated details of energy transport in high-density plasmas. Duston et al.[10] and Salzman, Szichman, and Krumbein[11] pointed out that x radiation might explain some previously unexplained experimental data with their simulation results. The experimental study of Ng and co-workers[13] showed that data were consistent with the x-radiation effect. Mochizuki et al.[12] showed the first experimental evidence of ionization burnthrough. However, few experiments have been presented to study details of energy transport especially for high-Z thin targets irradiated by a 263-nm laser.

Experimental studies are reported on energy transport by x radiation, shock, and electron thermal conduction through aluminum ($Z = 13$) and gold ($Z = 79$) thin foils irradiated with a frequency quadrupled Nd: glass ($\lambda = 263$ nm) laser beam. The measurement was conducted by observing the rear side emissions from the target with temporal resolution. For Al thin foils ($\leqslant 3\ \mu$m) emissions indicated that the energy transport mechanism could be primarily by the radiation front propagating at a slightly higher speed than the thermal conduction speed. Shock waves are clearly observed for Al targets thicker than 5 μm. For Au targets, a third peak could be distinctively observed in addition to the shock and thermal fronts, which was attributed to the radiation front.

II. EXPERIMENT

In the experiment, a 263-nm laser beam was focused with an $f/10$ optics onto the target metal foil (Al and Au) with normal incidence. Laser intensity was typically 6×10^{12} W/cm^2 with a 400-ps Gaussian pulse. The focal spot was 100 μm which contains 90% of the laser energy. The luminous emission ($\lambda = 300$–600 nm) of the target rear side was imaged onto the entrance slit of an S-20 streak camera. In order to know the time origin of the signal, a part of the incident laser pulse was introduced to the streak camera as a temporal fiducial mark. The emission intensity was calibrated *in situ* with a tungsten lamp and was converted to a blackbody temperature.[14]

Figures 1(a)–1(c) show temporally resolved emissions for Al foils of thicknesses of (a) 0.73, (b) 5.0, and (c) 8 μm,
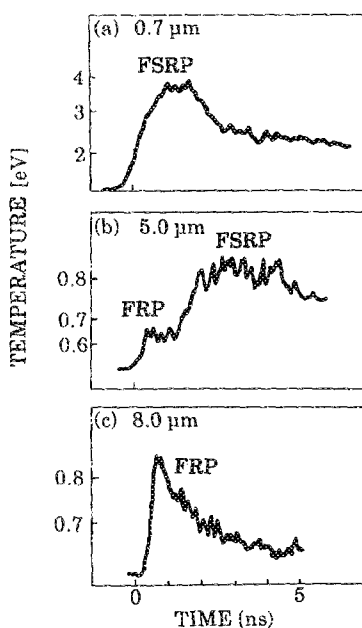

FIG. 1. Temporal histories of emissions (Al). (a) 0.73, (b) 5.0, and (c) 8.0 μm. A first slow rise peak (FSRP) is observed in (a). Both FSRP and the fast rise peak (FRP) are observed in (b), while only the FRP (shock) is seen in (c). A time of 0 ns corresponds to the laser intensity peak. The temperatures were obtained from emission intensities integrated over from 3000 to 6000 Å. The whole system was calibrated *in situ* with a tungsten lamp.

respectively. All were observed at a laser intensity of 6×10^{12} W/cm^2.

In Fig. 1(a) of the 0.73-μm Al case the emission intensity was very strong and the peak temperatures was around 4 eV. Since the rise time of the peak was rather slow (≈ 1 ns), we call this peak a first slow rise peak (FSRP). A second slow rise peak is shown in Fig. 2, when Au foil targets are used. After the FSRP was over, there was no other emission peak observed. This was checked using a slower time unit in the streak camera. When 5-μm Al was used [Fig. 1(b)], the temporal structure of the emission show two peaks: a fast rise ($\leqslant 200$ ps) peak (FRP) and the FSRP. The FSRP was about 1 ns delayed and the full width of half maximum (FWHM) seems to be two times wider than that of the FSRP in Fig. 1(a). The FSRP is due to the thermal front driven by the uv laser, which then relaxes after the irradiation.[14] Figure 1(c) shows a typical temporal emission shape of the shock break out (FRP) from the rear side of the target ($8\,\mu$m). The fast rise is also consistent with the shock wave. At this thickness the FSRP was about 10 ns after the laser peak and was not observed any more in this time range of the figure.

Observations for Au foil targets are shown in Figs. 2(a)–2(c). There are two components, both of which have slow rises in Fig. 2 (a), where a 1-μm Au foil was irradiated. The peak of the FSRP is out of the temporal range of the figure. The second slow rise peak (SSRP) appears at 1 ns after the laser peak. The rise time of the SSRP is again about 1 ns. The rise time of the FSRP is much slower than those of the Al cases [e.g., Fig. 1(a)]. This thermal front (FSRP) of Au should be retarded and should be spread out, since the areal mass density of Au is much larger (about seven times) than that of Al.

In Fig. 2(b), three components are clearly observed with a 3-μm Au foil. Just after the laser peak (~ 200 ps), there appears a third peak which has a fast rising slope. This

corresponds to the FRP in the Al cases, and again only the FSRP is observed when the thickness of the Au target is increased to 6 μm [Fig. 2(c)]. The SSRP also shows some relaxation compared to Fig. 2(a) and seem to be swallowed or absorbed by the FSRP.

III. DISCUSSION

There is a considerable difference between the emission structures from Al and Au targets. As shown in Fig. 2(b), the third peak (SSRP) is clearly observed only for Au targets, not for Al targets. For Au targets, most of the absorbed laser energy may be converted to soft x-ray energy (η_x/η_{abs} $\leqslant 80\%$.[3]) This strong x-ray flux should have an important role in the energy transport. As a matter of fact, we[12] reported that soft x rays could be transferred efficiently through a Au target via absorption resonance, or down-conversion. When a strong flux of x rays enters into a solid Au target, the Au target is ionized and then the ionization front may be formed. If the temperature in a front plasma increases, the absorption edges may shift to the high-energy side and then an optically thick plasma might become optically thin for x rays generated in that region. This is called the ionization burnthrough.[10] At the same time reemission of absorbed x rays may also occur. The efficiency of the reemission may become high for certain discrete shells such as O and N shell transitions. Thus, both ionization and reemission processes may well enhance the radiation energy transport, resulting in x-ray energies which could be transported for distances longer than the mean free path for a cold solid material. This kind of radiation front by an x-ray flux should be driven ahead of the ablation front and should only last for the duration of a laser pulse or slightly longer,[15] since the x rays generated by a laser pulse should have a pulse width almost the same as the laser pulse duration. After the laser pulse, the radiation front should decay, losing its driving force, and should be absorbed into a thermal front, which was first driven by the laser ablation and was then propagated by the heat conduction with its cooling temperature. In Figs. 2(a) and 2(b), the observed SSRP could correspond to the radiation front which should be observable more clearly for high-Z targets than for low- to mid-Z targets. The ionization speed could be estimated to be[12]

$$v_{\text{ion}} = 3\eta_{\text{ab}} I_x A^{2/3} m_p / 4\rho T^{4/3} = 1\text{–}2 \times 10^5 \text{ cm/s}, \qquad (1)$$

and is in reasonable agreement with the observed speed for the radiation front if the ablation speed is assumed to be smaller than the ionization front speed. Here η_{ab} is the absorption coefficient of the x-ray flux, I_x is the effective x-ray flux, ρ is the density of the target, m_p is the proton mass, and T is the electron temperature. For estimating the ionization speed, the electron temperature, the conversion efficiency of x radiation, and the absorption coefficient of the ionization front are taken to be 100 eV, 80% and 50%, respectively. Uncertainty of this estimated speed may vary within a factor of 2. Since the ablation speed is proportional to $1/\rho$ (ρ: material density) the ablation speed in a Au target could be almost one-seventh the ablation speed in Al, which could be $\approx 2 \times 10^4$ cm/s. Thus the separation between the radiation and ablation fronts becomes more pronounced for high-Z
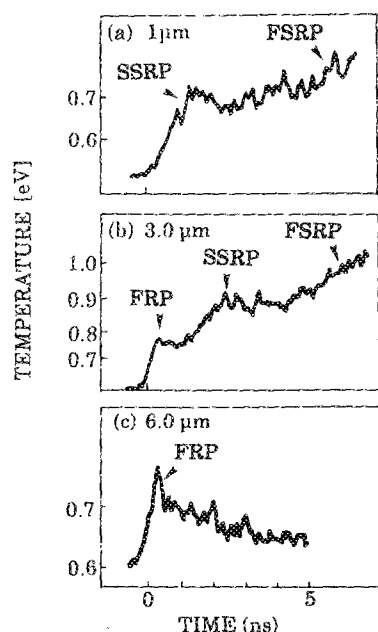

FIG. 2. Temporal histories of emissions (Au). (a) 1, (b) 3.0, (c) 6.0 μm. The two components, FSRP and the second slow rise peak (SSRP), both of which have slow rise times, are seen in (a). The three components, FRP, SSRP, and FSRP, are observed in (b), while only the FRP (shock) is seen in (c).
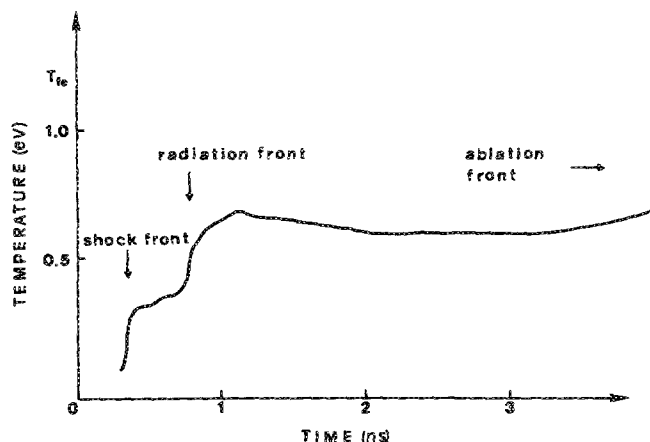
FIG. 3. Computer simulations by HIMICO. This simulation replicates well the observed rear emissions for Au targets. Clearly two (shock and radiation) fronts were observed.

FIG. 4. Ablation pressure vs flux intensity (W/cm^2). The estimated pressure for Al falls into the hatched region where previously reported data are indicated for a 263-nm laser irradiation. The pressure for Au appears to be higher and closer to the scaling by x-ray irradiation.

than for low- to mid-Z targets, consistent with the observed data (Figs. 1 and 2).

The experimental results are analyzed by comparison with a one-dimensional Lagrangian hydrodynamic code HI-MICO.[16] The simulation code includes the Thomas–Fermi EOS (equation of state) calculated by Latter[17] and Bell,[18] nonlocal thermodynamic equilibrium (LTE) atomic physics, multigroup radiation transport, and other conventional physics. For the opacity data, Kramer's formula was used with energy levels and populations calculated by a non-LTE average ion model.[19] This model has been proven[20] to produce results very close to the SESAME library[21] at high temperatures ($\geqslant 100$ eV) for xenon. Also used was the data of cold Au for lower temperatures given by Henke et al.[22] Details were reported in Ref. 23, where the x-ray transmission through Au thin foils was compared with experiments by examining the opacity calculations and its sensitivity to the results. The simulation replicates the laser absorption, the subsequent x-ray generation, and the transport. Therefore, the necessary inputs to the simulation are only the laser intensity, pulse shape, wavelength, and focusing angle, where other processes are self-consistently replicated in the code. The simulation result given in Fig. 3 corresponds to Fig. 2, but the target thickness was 0.5 μm. Three different phases are clearly seen in the figure: shock front, radiation front, and ablation front. If we increase the target thickness, both velocity and temperature of the radiation front increase in the simulation. Particularly at 0.75 μm the temperature increases up to 3 eV, which does not agree with the experimental result at 1 μm. This could be attributed to the reabsorption of the relatively high-energy radiation inside the target.[24] In this sense the absolute value of the opacity used in this calculation may be slightly larger than the experimental one or a two-dimensional effect may decrease the areal intensity of the deposited laser energy. The latter effect for the small spot size experiment such as our case should be non-negligible. The temperatures from these visible emissions may not represent the real blackbody temperature of the rear side plasma, since these visible emissions could only come from the very surface of the plasma where the tempera-
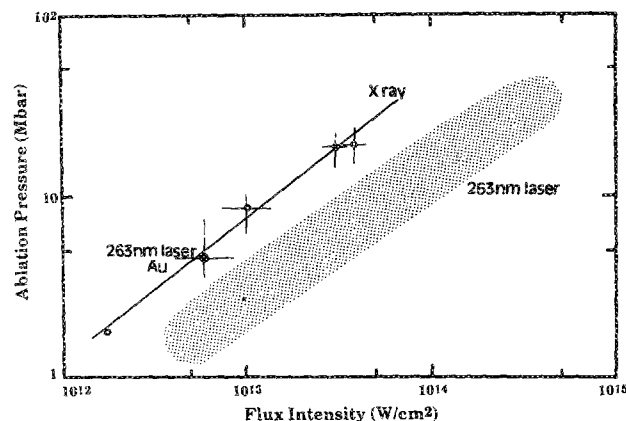
ture might be fairly low. This point was inferred from separate experiments, where both visible and x-ray rear emissions were observed of planar targets.[25] In this experiment the observed spectral region was from 300 to 600 nm. Thus we estimate that a real temperature at the front could range from 1 to 10 eV.

Finally ablation pressures may be estimated from the observed timing of the radiation (for Au) and the thermal (for Al) fronts for the given thickness of the targets. Results are shown in Fig. 4, where previously reported data by an x-ray flux driver[24,26] and uv laser ($\lambda = 263$ nm)[1,27] are shown as well. A value of 4 Mbar is obtained for Au at 6×10^{12} W/cm^2, and 1.5 Mbar for Al. While the ablation pressure for Al falls into the hatched region of uv laser data, the Au data fits onto the scaling by the x-ray driver. The results in the figure may indicate that the energy in a uv laser plasma is predominantly transported by soft x rays especially for a high-Z target such as Au.

IV. SUMMARY

In conclusion, energy transport was experimentally studied in Al and Au thin foils irradiated by a uv laser. Emissions from the rear side of the targets indicated that there was an emission peak due to soft x rays for Au targets. The results were well replicated in the simulation calculation. Estimated ablation pressure was also consistent with the energy being predominantly transported by soft x rays in the high-Z targets.

ACKNOWLEDGMENTS

[1] R. Fabbro, E. Fabre, F. Amiranoff, C. Labaune, J. Virmont, and M. Weinfeld, Phys. Rev. A 26, 2289 (1982); R. Fabbro, B. Faral, F. Cottet, and J. P. Romain, J. Appl. Phys. 56, 3204 (1984); F. Cottet, J. P. Romain, R. Fabbro, and B. Faral, Phys. Rev. Lett. 52, (1984).
[2] R. E. Turner, K. Estabrook, R. L. Kauffman, D. R. Bach, R. P. Drake, D. W. Phillion, D. F. Lasinski, E. M. Campbell, W. L. Kruer, and E. Williams, Phys. Rev. Lett. 54, 689 (1985).

5070   J. Appl. Phys., Vol. 65, No. 12, 15 June 1989

Tanaka et al.   5070

[3]R. Kodama, K. Okada, N. Ikeda, M. Mineo, K. A. Tanaka, T. Mochizuki, and C. Yamanaka, J. Appl. Phys. **59**, 3050 (1986).

[4]P. Alaterre, H. Pepin, R. Fabbro, and B. Faral, Phys. Rev. A **34**, 4184 (1986).

[5]W. C. Mead, E. M. Campbell, K. G. Estabrook, R. E. Turner, W. L. Kruer, P. H. Y. Lee, B. Pruett, V. C. Rupert, K. G. Tirsell, H. G. L. Stradling, F. Ze, C. E. Max, and M. D. Rosen, Phys. Rev. Lett. **47**, 1289 (1981).

[6]H. Nishimura, F. Matsuoka, M. Yagi, K. Yamada, S. Nakai, G. H. McCall, and C. Yamanaka, Phys. Fluids **26**, 1688 (1983).

[7]W. C. Mead, P. H. Y. Lee, B. Pruett, V. C. Rupert, K. G. Tirsell, G. L. Stradling, F. Ze, C. E. Max, M. D. Rosen, and B. F. Lasinski, Phys. Fluids **26**, 2316 (1983).

[8]E. A. McLean, S. H. Gold, J. A. Stamper, R. R. Whitlock, H. R. Griem, S. P. Obenschain, B. H. Ripin, S. E. Bodner, M. J. Herbst, S. J. Gitomer, and M. K. Matzen, Phys. Rev. Lett. **45**, 1246 (1980).

[9]G. Thiell, B. Meyer, P. Aussage, and X. Fortin, Opt. Commun. **46**, 305 (1983).

[10]D. Duston, R. W. Clark, J. Davis, and J. P. Apruzese, Phys. Rev. A **27**, 1441 (1983).

[11]D. Saltzmann, H. Szichman, and D. Krumbein, Phys. Fluids **30**, 515 (1987).

[12]T. Mochizuki, K. Mima, N. Ikeda, R. Kodama, H. Shiraga, K. A. Tanaka, and C. Yamanaka, Phys. Rev. **36**, 3279 (1987).

[13]A. Ng, D. Parfeniuk, L. DaSilva, D. Pasini, Phys. Fluids **28**, 2915 (1985).

[14]A. Yamauchi, K. A. Tanaka, M. Kado, R. Kodama, T. Mochizuki, T. Yamanaka, S. Nakai, and C. Yamanaka, Appl. Phys. Lett. **52**, 786 (1988).

[15]N. Ikeda, K. A. Tanaka, K. Okada, T. Mochizuki, and C. Yamanaka, Rev. Sci. Instrum. **57**, 2489 (1986).

[16]T. Yabe and C. Yamanaka, Comments Plasma Phys. Controlled Fusion **9**, 169 (1985).

[17]R. Latter, Phys. Rev. **99**, 1584 (1955).

[18]A. R. Bell, "New Equation of State for MEDUSA," Rutherford Laboratory Report No. RL-80-091 (1981) (unpublished).

[19]S. Kiyokawa, T. Yabe, and T. Mochizuki, Jpn. J. Appl. Phys. **22**, L772 (1983); M. Itoh, T. Yabe, and S. Kiyokawa, Phys. Rev. A **35**, 233 (1987).

[20]T. Yabe and B. Goel, Jpn. J. Appl. Phys. **26**, L296 (1987).

[21]W. F. Huebner, A. L. Merts, N. H. Magee, Jr., and M. F. Argo, Astrophysical Opacity Library, Los Alamos Scientific Laboratory, Report No. LA-6760 M (1977) (unpublished).

[22]B. L. Henke, P. Lee, T. J. Tanaka, R. L. Shimabukuro, and B. K. Fujikawa, At. Data Nucl. Data Tables **27**, 1 (1982).

[23]T. Yabe, S. Kiyokawa, H. Nishimura, and C. Yamanaka, Jpn. J. Appl. Phys. **24**, L439 (1985).

[24]T. Yabe, S. Kiyokawa, T. Mochizuyki, S. Sakabe, and C. Yamanaka, Jpn. J. Appl. Phys. **22**, L88 (1983).

[25]R. Kodama and K. A. Tanaka (to be published).

[26]T. Endo, H. Shiraga, K. Shihoyama, and K. Kato, Phys. Rev. Lett. **60**, 1022 (1988).

[27]T. Boehly, K. A. Tanaka, T. Mochizuki, and C. Yamanaka, J. Appl. Phys. **60**, 3840 (1986).